Two Distinct MUS81-EME1 Complexes from Arabidopsis Process Holliday Junctions[1][W]

Verena Geuting[2], Daniela Kobbe, Frank Hartung, Jasmin Dürr[3], Manfred Focke, and Holger Puchta*

Botanik II, Universität Karlsruhe, 76128 Karlsruhe, Germany

The MUS81 endonuclease complex has been shown to play an important role in the repair of stalled or blocked replication forks and in the processing of meiotic recombination intermediates from yeast to humans. This endonuclease is composed of two subunits, MUS81 and EME1. Surprisingly, unlike other organisms, Arabidopsis (*Arabidopsis thaliana*) has two *EME1* homologs encoded in its genome. AtEME1A and AtEME1B show 63% identity on the protein level. We were able to demonstrate that, after expression in *Escherichia coli*, each EME1 protein can assemble with the unique AtMUS81 to form a functional endonuclease. Both complexes, AtMUS81-AtEME1A and AtMUS81-AtEME1B, are not only able to cleave 3′-flap structures and nicked Holliday junctions (HJs) but also, with reduced efficiency, intact HJs. While the complexes have the same cleavage patterns with both nicked DNA substrates, slight differences in the processing of intact HJs can be detected. Our results are in line with an involvement of both MUS81-EME1 endonuclease complexes in DNA recombination and repair processes in Arabidopsis.

DNA is constantly damaged by extrinsic and intrinsic factors, such as UV and ionizing irradiation, chemicals, and cellular processes. The accumulation of DNA damage can impair essential processes, including transcription and replication, and can induce aberrant chromosome structures. Branched DNA can lead to chromosome missegregation in mitosis or meiosis. To overcome this kind of DNA damage and to maintain a stable genomic structure, organisms have developed a complex network of signal transduction pathways and DNA repair mechanisms. These repair pathways involve the recognition and subsequent removal of DNA lesions (Tuteja et al., 2001; Ciccia et al., 2008). In addition to helicases and topoisomerases (Hartung et al., 2007a, 2007b; Kobbe et al., 2008), structure-specific nucleases are often involved in the proper resolution of irregular DNA structures like 3′-flaps, Holliday junctions (HJs), and stalled or blocked replication forks. HJ resolvases that process the four-way branched structures that form during homologous recombination, and related repair processes fall into this category (Nishino et al., 2006). The MUS81 protein belongs to the XPF/MUS81 family of nucleases and forms a functional endonuclease complex with its interaction partner EME1 (also referred to as MMS4 in *Saccharomyces cerevisiae*; Boddy et al., 2000; Interthal and Heyer, 2000; Chen et al., 2001). This protein complex has been shown to play an important role in DNA repair in human, yeasts, and Drosophila (*Drosophila melanogaster*), especially in dealing with stalled and collapsed replication forks and in the processing of recombination intermediates. The loss of one of the proteins, MUS81 or EME1 (or MMS4), causes these organisms to have an increased sensitivity to DNA damaging agents (Boddy et al., 2000, 2001; Interthal and Heyer, 2000; Abraham et al., 2003; Odagiri et al., 2003; McPherson et al., 2004; Hanada et al., 2006).

While the MUS81 endonuclease is highly conserved in eukaryotes, its role in meiosis differs. The loss of *MUS81* causes a complete loss of spore viability in *Schizosaccharomyces pombe*, whereas the respective mutant is partially fertile in *S. cerevisiae* and fully fertile in mammals. In contrast with *S. pombe*, where MUS81-EME1 is essential for the processing of recombination intermediates, *S. cerevisiae* and mammals possess at least one additional alternative pathway, which is linked to the MSH4-MSH5 complex, for cross-over (CO) formation (de los Santos et al., 2001; Osman et al., 2003; Whitby, 2005; Holloway et al., 2008). Recently, it was shown that HsGEN1 and ScYEN1 can resolve HJs, and their involvement in an alternative pathway to MUS81 was suggested (Ip et al., 2008).

Recombinantly expressed protein complexes of MUS81-EME1 (or -MMS4) versus native protein extract preparations differ especially in their ability to cleave an intact HJ, the central recombination intermediate. It has been speculated that the presence of activating factors or posttranslational modifications in

[1] This work was supported by the European Union Sixth Framework Programme STREP TAGIP (LSHG–CT–2005–018785).

[2] Present address: Radiation Biology and DNA Repair, Darmstadt University of Technology, 64287 Darmstadt, Germany.

[3] Present address: Institut für Forstbotanik und Baumphysiologie, Albert-Ludwigs-Universität, 79110 Freiburg, Germany.

* Corresponding author; e-mail holger.puchta@bio.uka.de.

The author responsible for distribution of materials integral to the findings presented in this article in accordance with the policy described in the Instructions for Authors (www.plantphysiol.org) is: Holger Puchta (holger.puchta@bio.uka.de).

[W] The online version of this article contains Web-only data.

www.plantphysiol.org/cgi/doi/10.1104/pp.109.136846

the native protein extracts was causing these differences (Doe et al., 2002; Gaillard et al., 2003). In any case, the respective MUS81 endonuclease complexes can cleave different synthetic DNA substrates in vitro, like 3′-flaps, replication fork structures, D-loops, and nicked HJs (Boddy et al., 2001; Chen et al., 2001; Kaliraman et al., 2001; Constantinou et al., 2002; Doe et al., 2002; Abraham et al., 2003; Ciccia et al., 2003; Gaillard et al., 2003; Osman et al., 2003; Fricke et al., 2005; Taylor and McGowan, 2008). Recently, the group of Whitby detected cleavage activity of an intact HJ with recombinant MUS81 endonuclease complexes from *S. cerevisiae* and *S. pombe*. This activity was shown to be dependent on the oligomerization of the respective dimeric endonuclease complexes to tetrameric complexes, each consisting of two MUS81 and EME1 (MMS4) subunits (Gaskell et al., 2007; Taylor and McGowan, 2008). By interaction studies, it was shown before, that HsEME1 as well as HsMUS81 oligomerize, indicating the existence of oligomeric complexes (Blais et al., 2004). The observations are consistent with the proposed nick-counternick mechanism for processing an intact HJ in the presence of two active sites (Gaillard et al., 2003).

We previously identified a functional homolog (*AtMUS81*) of *MUS81* in the genome of Arabidopsis (*Arabidopsis thaliana*; Hartung et al., 2006). As in yeast, mutations in *AtMUS81* result in a strong sensitivity to the genotoxic agents mitomycin C, methylmethane sulfonate (MMS), cis-platin, and ionizing radiation (Hartung et al., 2006; Berchowitz et al., 2007). In addition, the mutant is deficient in homologous recombination after the induction of genotoxic stress (Hartung et al., 2006). Together, these results indicate that AtMUS81 functions in homologous recombination repair in somatic cells and in the repair of collapsed replication forks. Synthetic lethality has been observed for *MUS81* mutations combined with a mutation in RECQ helicase in Arabidopsis *mus81/recq4A*, indicating that both proteins function in alternative pathways for processing recombination intermediates (Hartung et al., 2006). This has also been shown for *S. cerevisiae*, *S. pombe*, and *D. melanogaster* (Boddy et al., 2000; Mullen et al., 2001; Trowbridge et al., 2007). *AtMUS81*-deficient mutants are fertile but have impaired pollen viability and a reduction in meiotic COs (Berchowitz et al., 2007). As in *S. cerevisiae*, the existence of two independent CO pathways in Arabidopsis has been proposed to involve either the MUS81 endonuclease (class II) or the MSH4-MSH5 complex (class I; Copenhaver et al., 2002; Higgins et al., 2008). The latter is supposed to be predominant, as *Atmsh4* mutants show an 85% reduction in chiasmata frequency during metaphase I (Higgins et al., 2008).

Interestingly, two *EME1* homologs exist in the Arabidopsis genome. Several EME1 proteins are also found in humans; however, in that case, only a single gene was identified (Blais et al., 2004). It was also reported that a more distantly related homolog, HsEME2, interacts with HsMUS81 and displays 3′-flap nuclease activity (Ciccia et al., 2007). The *AtEME1A* and *AtEME1B* homologs in Arabidopsis share about 63% identity on the protein level. In this work, using proteins expressed in *Escherichia coli*, we address the question of whether both homologs of EME1, AtEME1A and AtEME1B, form two enzymatically active endonuclease complexes with the interaction partner AtMUS81 and whether AtMUS81-AtEME1A and AtMUS81-AtEME1B differ in their enzymatic activities.

RESULTS

Identification of Two EME1 Homologs in Arabidopsis: *AtEME1A* and *AtEME1B*

We were able to identify two EME1 homologs in Arabidopsis, *AtEME1A* and *AtEME1B* (At2g21800 and At2g22140). Both genes are encoded on chromosome 2 and lie in close proximity to each other (separated by only 110 kb), indicating that they arose by a recent segmental duplication. According to our database searches, duplicated EME1 genes are not present in plants outside the Brassicaceae, namely, moss (*Physcomitrella patens*), rice (*Oryza sativa*), and poplar (*Populus* spp.). Due to the high homology between the two genes, the ancestral *AtEME1* was most probably duplicated approximately 40 million years ago, approximately around the time of the origin of the Brassicaceae. The last of three paleopolyploidic phases in *Brassica* ancestors has been located to this time by comparative genomic investigations (Schranz and Mitchell-Olds, 2006). Performing a database search, we could also find the duplicated genes in the very recently sequenced genome of *Arabidopsis lyrata*, a close relative of Arabidopsis, which supports the above described hypothetical time point of origin (Joint Genome Institute accession nos. are fgenesh1_pg.C_scaffold_4000112 and gw1.4.853.1).

By analyzing the cDNAs that are encoded by both genes, we could confirm the sequence of the RAFL14-53-G19 clone (AK228007) for *AtEME1A*, except for an alternative splicing event at exon 6. Exon 6 in our cDNA starts nine nucleotides earlier; therefore, the predicted protein is 549 amino acids in size, instead of 546 amino acids, as suggested by AK228007. For *AtEME1B*, we identified a coding sequence that is mostly consistent with the predicted one (NM_127782), though it possesses one more exon; therefore, it consists of 12 exons and a total coding length of 1,656 bp. According to our reverse transcription (RT)-PCR experiments, the *AtEME1B* transcript consists of 1830 nucleotides and harbors a 5′-untranslated region (UTR) of 51 nucleotides and a 3′-UTR of 123 nucleotides (accession no. FJ161970). The resulting protein is 551 amino acids in size.

The complete protein sequences are 62.7% identical (Fig. 1); at the DNA level, there is 75.4% identity within the coding regions. In such a gene pair, we would expect that there be higher identity on the protein level

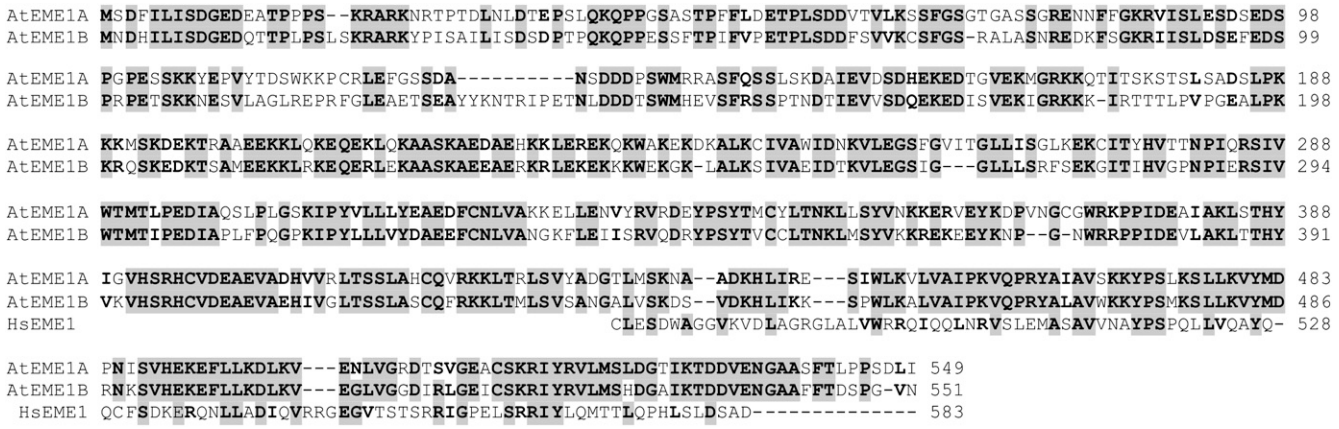

Figure 1. Full-length sequence alignment of both Arabidopsis EME1 proteins and the C-terminal part of HsEME1. Identical amino acids that occur at least in two of the three sequences are shaded and in bold. Conservative amino acid substitutions are in bold without shading. For the human EME1 protein, only the conserved C-terminal part, amino acids 473 to 583, is shown. Conservative amino acid substitutions are: D to E; K to R; and I to V or L. The respective amino acid position of each sequence is given on the right.

than on the DNA level due to the flexibility in the third position of most triplets (wobble base). Instead, there are more mutations that change the coding triplet to a different amino acid than silent mutations in the wobble position of a triplet; therefore, both genes must rapidly evolve by hypermutation. This fact alone may indicate that AtEME1A and AtEME1B have divergent functions. By comparing the coding sequences of the two homologs, we detected a total of seven insertions/deletions (varying in size from 3 to 30 nucleotides). These were all triplet or multiple triplet InDels; therefore, the phase of the respective open reading frames (ORFs) is conserved in all cases. When considering the entire genes, including intron and UTR sequences, there is 55.9% identity between *AtEME1A* and *AtEME1B*. Both genes possess a total of 11 introns; all of these are located at identical positions with respect to their translated coding region (for other instances, see Hartung et al., 2002). The transcript level of both genes was compared by real-time PCR in different tissues (roots, stem, leaf, and flowers) and found to be always lower than that of *AtMUS81*. On average, the transcript level of *AtEME1A* was 2-fold higher than *AtEME1B* in the roots, 4-fold higher in flowers, identical in the stems, and 2-fold lower in the leaves. The difference of the transcript level of both EME1 genes to the transcript level of *AtMUS81* is 2- to 11-fold in the respective tissues (Supplemental Table S1).

In a protein alignment using full-length proteins of AtEME1A, AtEME1B, HsEME1, ScMMS4, and SpEME1, both of the Arabidopsis proteins were found to be only 10% to 13% identical to the human and yeast proteins. Nevertheless, HsEME1, ScEME1, and SpEME1 have the same low level of homology to each other (10%–15%). The most conserved region is located in the C-terminal part of the protein. Here, AtEME1A and AtEME1B were found to possess 25% and 26% identity to the human EME1 protein, respectively (Fig. 1, bottom part).

The structure of Arabidopsis MUS81 has been described previously. Briefly, the protein contains three domains: the conserved ERCC4 endonuclease domain with the catalytic center, the polymerase β-domain (N-terminal), which contains one of the two helix hairpin helix domains, and a domain similar to the RUVA C-terminal domain that is not found in other MUS81 proteins (Hartung et al., 2006).

Purification of AtMUS81-AtEME1A/1B and AtMUS81 (D470-471A)-AtEME1A/1B Endonuclease Complexes

In this work, recombinant protein expression produced an AtMUS81 protein with a molecular mass of 75.5 kD (with N-terminal His-tag), an AtEME1A protein of 62.9 kD, and an AtEME1B protein of 63.8 kD (with C-terminal StrepII-tag).

Our initial experiments showed that the complexes comprised of individually purified subunits are not enzymatically active. Thus, the coexpression of AtMUS81 with its respective interaction partner, AtEME1A or AtEME1B, was found to be necessary to allow for the immediate heterodimeric complex formation upon expression. This practice has been shown to be required for the enzymatic activity of eukaryotic XPF/MUS81 family proteins in other organisms (Boddy et al., 2001; Ciccia et al., 2003, 2008; Nishino et al., 2003).

The purification of the recombinant protein complexes from *E. coli* was performed using double affinity chromatography with the help of the StrepII-tag (StrepTactin chromatography) and the His-tag (Cu^{2+}-IMAC). Due to the fact that the purification was performed with the affinity tag of the respective interaction partner AtMUS81 and AtEME1A or AtEME1B,

the consecutive purification procedure is a suitable in vitro method of demonstrating the interaction between both complex partners. Furthermore, the monomer excess was removed, so that stochiometric amounts of both interaction partners could be detected in the final fractions. The purified protein complexes migrated as double bands of expected size on colloidal Coomassie-stained SDS-PAGE gels, except for the AtEME1B protein, which exhibits a lower electrophoretic mobility than expected (Supplemental Fig. S1).

It was shown that the Asp residues in the catalytic center of SpMUS81 are essential for its function, but not for the interaction with SpEME1 (Boddy et al., 2001). Therefore, we used constructs with a mutated form of AtMUS81 [amino acid sequence of the catalytic center AERKXX(D470A)(D471A)] as negative controls. Following the same procedure as above, we were able to purify complexes with both AtEME1 proteins, AtMUS81(D470-471A)-AtEME1A and AtMUS81 (D470-471A)-AtEME1B, respectively.

AtMUS81-AtEME1A and AtMUS81-AtEME1B Display Endonucleolytic Activity on a 3′-Flap Substrate

With a 3′-flap structure we could show that both homologous endonuclease complexes but not those with AtMUS81(D470-471A) display endonucleolytic activity. For the endonucleolytic activity of both AtMUS81-AtEME1A and AtMUS81-AtEME1B, the standard divalent cation Mg^{2+} can be replaced by Ca^{2+}. Mn^{2+} supports activity as a cofactor to a higher extent and leads to the formation of further cleavage products of lower molecular mass; Ni^{2+} and Zn^{2+} cannot serve as cofactors for catalytic activity (Fig. 2).

Both negative control protein complexes AtMUS81 (D470-471A)-AtEME1A and AtMUS81(D470-471A)-AtEME1B lacked enzymatic activity with all metal ions, demonstrating the absence of enzymatic contaminations and, therefore, the high quality of the purification.

As the cleavage of HJs by MUS81 endonuclease complexes is an important question, we standardized the amount of MUS81-EME1A and -EME1B complexes used in the assays to the same rate of activity with the nicked static HJ nXO. With this standardization, a higher activity with the 3′-flap substrate was observed for AtMUS81-AtEME1B than for AtMUS81-AtEME1A. Repeated experiments using both denaturing sequencing gels and native PAGE validated this result.

It was observed that the cleavage fragments accumulate with increasing incubation time. For the processing of the 3′-flap, two main sites of endonucleolytic cleavage could be detected for both homologous complexes located at three and four nucleotides in 5′ direction of the branch point of the flap (Fig. 3, B and C). Several further cleavage sites were found to be located within five to seven nucleotides 5′ of the branch point, though to a lesser extent (Fig. 3, A and B).

Recombinant AtMUS81-AtEME1 Endonuclease Complexes Are Able to Cleave Intact HJs

There are important differences in the ability to cleave intact HJs between native and recombinant MUS81-EME1 or MUS81-MMS4 protein extracts in yeasts and mammals. In this study, we tested the static HJ structure, specifically the intact (XO) and nicked (nXO) HJ without sequence homologies at the CO point. Amounts of AtMUS81-AtEME1A and AtMUS81-AtEME1B that displayed the same rate of activity on the nXO substrate were used to compare XO cleavage of both homologous complexes. Remarkably, both recombinant AtMUS81-EME1A and AtMUS81-EME1B complexes can cleave the intact HJ; however, the nXO

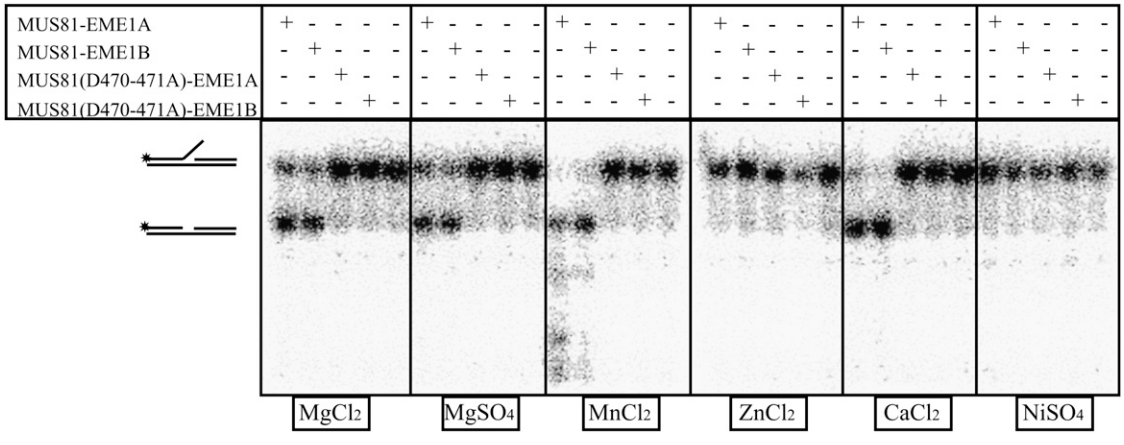

Figure 2. Effect of different divalent metal ions on the enzymatic activity of AtMUS81-AtEME1A and AtMUS81-AtEME1B. Autoradiography of a native PAGE gel. Ten nanograms of AtMUS81-AtEME1A or AtMUS81-AtEME1B and AtMUS81(D470-471A)-AtEME1A or AtMUS81(D470-471A)-AtEME1B, respectively, were incubated with the 3′-flap substrate for 30 min. $MgCl_2$ was substituted by $MgSO_4$, $MnCl_2$, $ZnCl_2$, $CaCl_2$, and $NiSO_4$ at a concentration of 2.5 mM. DTT was omitted from the reactions. Substrate and product are shown on the left. The asterisk marks the ^{32}P label.

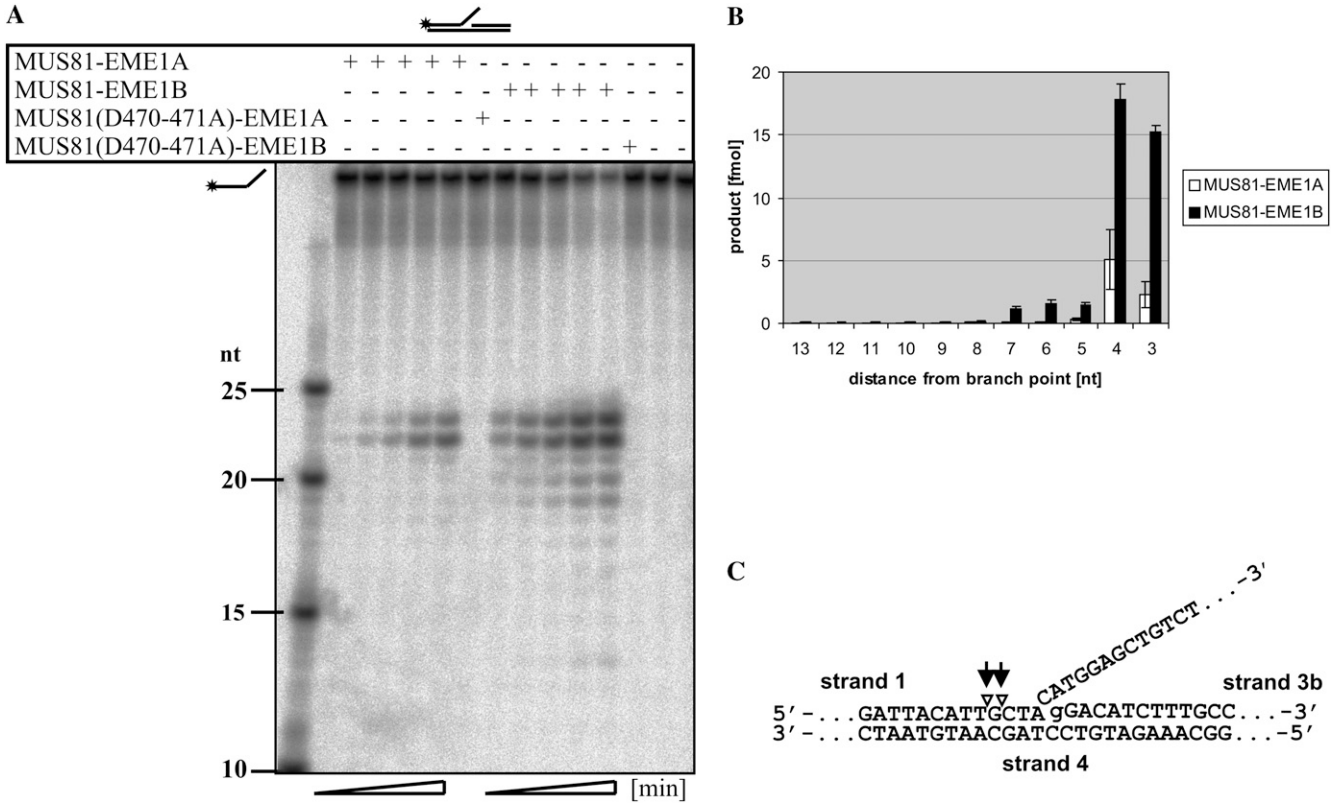

Figure 3. Processing of the 3′-flap structure by AtMUS81-AtEME1A and AtMUS81-AtEME1B. Representative autoradiography. The 3′-flap substrate was incubated with AtMUS81-AtEME1A or AtMUS81-AtEME1B as indicated in "Materials and Methods." A, Reactions were analyzed on a 20% denaturing TBE-urea (7 M) sequencing gel; the sizes of cleavage fragments are given in nucleotides. B, After quantification of the respective cleavage fragments, the positions of endonucleolytic cleavages were mapped. The endonuclease data represent the mean of three independent experiments. C, Structure and sequence of the 3′-flap substrate with the corresponding cleavage sites of AtMUS81-AtEME1A (white arrowheads) and AtMUS81-AtEME1B (black arrows).

served as a better substrate for both of the homologous complexes and was cut with higher efficiency than the XO (Fig. 4A). The endonuclease activity was optimal for the XO substrate at a range of 1 mM Mg^{2+} for both of the homologous complexes; a decrease in activity was observed at higher concentrations. In contrast, increasing activity for both complexes was observed with nXO with increasing Mg^{2+} concentrations (data not shown).

Positions of Endonucleolytic Cleavage of the HJ Structure Substrates

To map the positions of endonucleolytic cleavage, the XO and nXO structures were prepared with a radioactive label in different composing strands; time-course experiments were then performed. For the nXO with a nick in strand 3, the main cleavage product corresponded to a cleavage site at four nucleotides in the 5′ direction of the junction point in the first duplex arm for AtMUS81-AtEME1A and AtMUS81-AtEME1B (Fig. 4A). No cleavage products were detected by denaturing PAGE using the nXO structures labeled on the second and fourth duplex arm. However, using native PAGE, comparable activity could be observed for both homologous complexes with differently labeled nXO substrates. These results indicate that the nicked HJ is exclusively cut in the opposing strand (strand 1) of the nick (strand 3) near the junction point (Fig. 5); this cleavage results in linear duplex products with gaps and short 5′-flaps.

Processing of XO was detected in all four duplex arms, ranging from 3 to 13 nucleotides 5′ of the junction point for both AtMUS81-AtEME1A and AtMUS81-AtEME1B (Fig. 4). The main cleavage sites were four nucleotides 5′ of the junction point in three of the four duplex arms (XO-2/-3/-4) for AtMUS81-AtEME1A. For AtMUS81-AtEME1B, the main cleavage sites were less defined, being located between 3 and 13 nucleotides 5′ of the junction point at intervals of single nucleotides. The major cleavage site in strand 2 is offset by one nucleotide for the two homologous complexes. For both AtMUS81-AtEME1A and AtMUS81-AtEME1B, almost no cleavage was detected

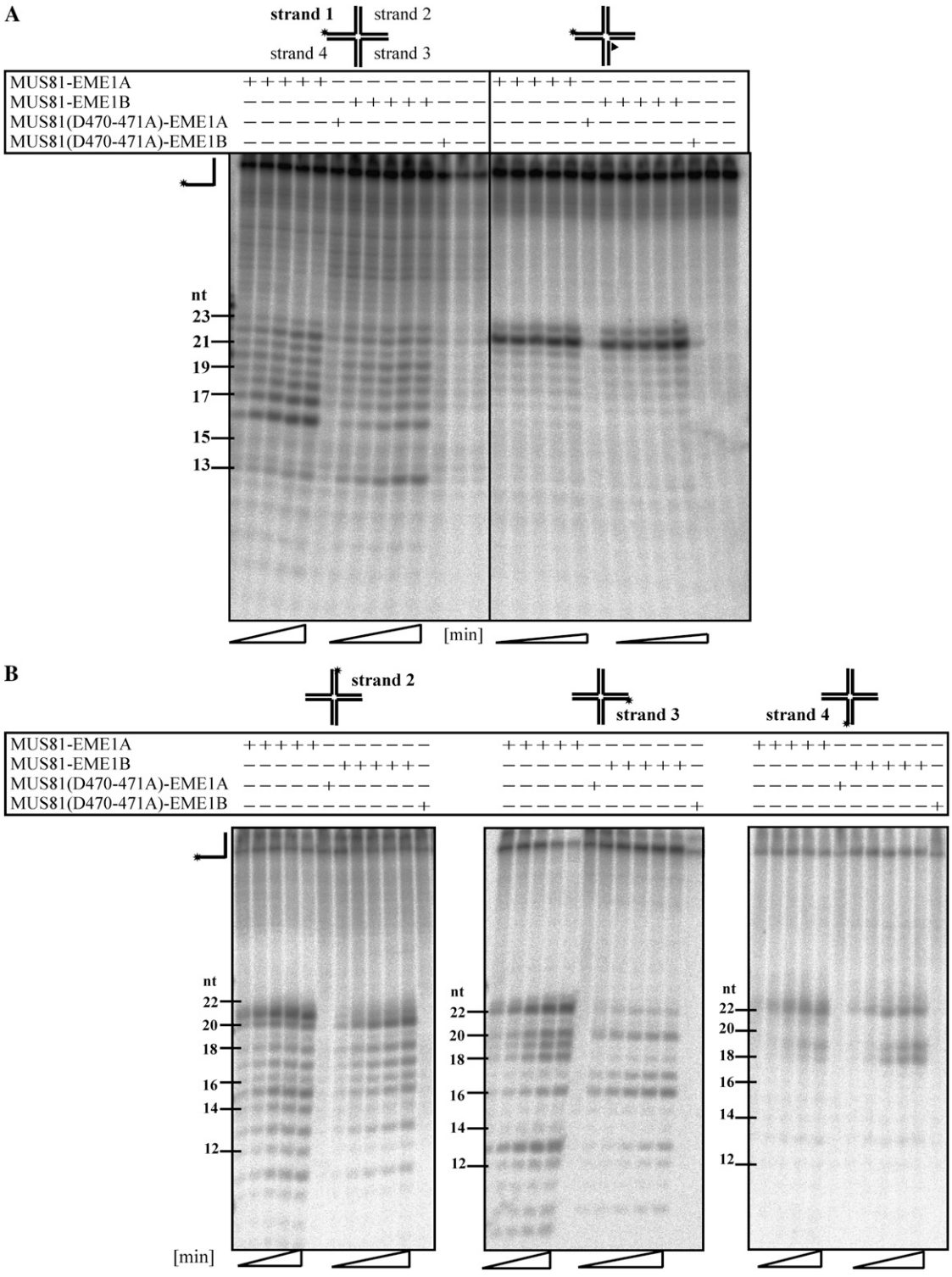

Figure 4. Cleavage of intact and nicked HJs (XO/nXO) by AtMUS81-AtEME1A and AtMUS81-AtEME1B. Representative autoradiography. The nXO or XO substrates were incubated with AtMUS81-EME1A or AtMUS81-EME1B as indicated in "Materials and Methods." Reactions were analyzed on a 20% denaturing TBE-urea (7 M) sequencing gel; the sizes of cleavage fragments are given in nucleotides. A, Time-course experiments with XO-1 and nXO-1; samples were run on the same gel; the arrowhead marks the nick in strand 3. B, Time-course experiments with XO-2, XO-3, and XO-4.

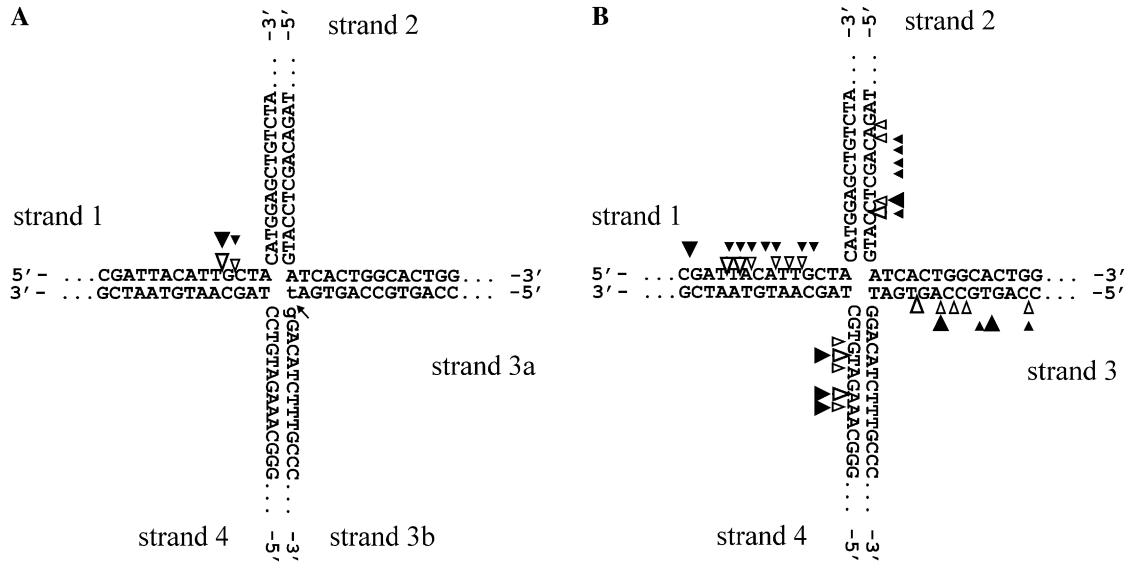

Figure 5. Positions of endonucleolytic cleavage on each duplex arm of the intact and nicked HJ structure. The respective cleavage sites of AtMUS81-AtEME1A (white arrowheads) and AtMUS81-AtEME1B (black arrowheads) three and four nucleotides 5′ of the junction point in the first duplex arm of nXO (A) or in each duplex arm of XO (B) are shown. The arrow marks the nick in the nXO. Small arrowheads: 5% to 15% of the overall product. Big arrowheads: 15% to 65% of the overall product. Results are from three independent experiments.

at positions 11 and 12 nucleotides 5′ of the junction point or in the 3′ direction in any duplex arm (Fig. 5).

DISCUSSION

The MUS81 endonuclease complex from yeasts and mammals is involved in several DNA repair processes, such as the processing of irregular replicative recombination intermediates, the restarting of stalled and blocked replication forks, and meiotic recombination. Recent investigations into insertion mutants of *MUS81* in Arabidopsis have confirmed that its function is conserved in plants as well (Copenhaver et al., 2002; Hartung et al., 2006; Berchowitz et al., 2007; Higgins et al., 2008).

We were able to verify the existence and expression of two EME1 homologs in Arabidopsis, and the question arose as to whether indeed two active nuclease complexes could be formed and whether both complexes have identical biochemical specificities. No in vivo analysis of these proteins has yet been published, perhaps because insertion mutants are not available for both genes in the same Arabidopsis cultivar in the public mutant libraries and Arabidopsis cultivars might differ in their repair and recombination behaviors. The fact that the two genes are only about 110 kb apart makes it extremely difficult to obtain a double mutant by crossing insertion mutants of both genes.

The recombinant coexpression of AtMUS81 and AtEME1A or AtEME1B in *E. coli* should facilitate heterodimeric complex formation of both interaction partners right after expression, which is required for endonucleolytic activity (Boddy et al., 2001; Ciccia et al., 2003, 2008; Nishino et al., 2003). No catalytic activity could be obtained by mixing separately purified recombinant complex partners, as has already been shown for human MUS81-EME1 (Ciccia et al., 2003). Other accessory factors might be involved in the formation of functional endonuclease complexes. The interaction of AtMUS81 and the respective AtEME1 homolog could be confirmed using double affinity chromatography. We were able to show that both homologous endonuclease complexes AtMUS81-AtEME1A and AtMUS81-AtEME1B display endonucleolytic activity.

For AtMUS81-AtEME1A and AtMUS81-AtEME1B, both Mg^{2+} and Ca^{2+} were able to serve as cofactors. In contrast, for ScMUS81-MMS4, Ca^{2+} supported binding of a HJ but prevented its cleavage (Fricke et al., 2005; Gaskell et al., 2007; Ehmsen and Heyer, 2008). Mn^{2+}, though at a nonphysiological concentration, supported enzymatic activity in both homologous complexes and even resulted in a higher specific activity and additional cleavage products, as is true for ScMUS81-MMS4 (Fricke et al., 2005; Ehmsen and Heyer, 2008). The lack of endonucleolytic activity of AtMUS81 (D470-471A)-EME1A and AtMUS81(D470-471A)-EME1B demonstrates the high quality of purification and the absence of contaminating *E. coli* proteins that may have been activated by different metal ions.

AtMUS81-AtEME1A and AtMUS81-AtEME1B were able to process a 3′-flap structure, as has been shown for all characterized MUS81 endonuclease complexes

(Kaliraman et al., 2001; Constantinou et al., 2002; Ciccia et al., 2003; Fricke et al., 2005). A higher specific activity was detected for AtMUS81-AtEME1B than AtMUS81-AtEME1A, supporting the existence of a substrate preference. Both complexes cut at the same positions, which also correspond to those of SpMUS81-EME1 and ScMUS81-MMS4 (Bastin-Shanower et al., 2003; Gaillard et al., 2003; Whitby et al., 2003). The 3′-flaps occur during homologous recombination repair of double strand breaks according to the synthesis dependent strand annealing model, as well as to the strand displacement-mediated CO model (de los Santos et al., 2003; Puchta, 2005) if the newly synthesized strand is longer than the 3′ single-stranded tail on the other side of the break. Failure to cleave these 3′-flaps results in unprocessed recombination intermediates and can also impede dHJ formation as CO precursors (de los Santos et al., 2003; Oh et al., 2008).

The observed colocalization of AtMUS81 with the initiating recombination protein AtRAD51 in the nuclei of pollen mother cells (Higgins et al., 2008) and the processing of the 3′-flap shown in this work point to an early function of the MUS81 endonuclease complexes in meiotic homologous recombination processes in Arabidopsis, as has been proposed for ScMUS81-MMS4 (Oh et al., 2008).

The HJ is a central recombination intermediate, not only in meiosis, but also during repair of double strand breaks and in the restart of blocked or collapsed replication forks. The ability of native and recombinant preparations to cleave intact HJs has been shown to vary. Recombinant MUS81-EME1 or -MMS4 complexes from mammals (Ciccia et al., 2003; Taylor and McGowan, 2008) and yeasts (Kaliraman et al., 2001; Doe et al., 2002; Gaillard et al., 2003; Osman et al., 2003; Fricke et al., 2005) show no or only weak cleavage of intact HJs, whereas the respective native preparations can partially cleave intact HJs (Boddy et al., 2001; Chen et al., 2001; Constantinou et al., 2002; Ciccia et al., 2003; Gaillard et al., 2003). This disagreement was discussed to be due to the presence of activating protein factors or posttranslational modifications in the native extracts (Doe et al., 2002; Gaillard et al., 2003).

Recently, however, the oligomerization of the endonuclease complexes was found to influence the processing of intact HJs. The group of Whitby obtained efficient HJ cleavage with recombinant ScMUS81-MMS4 and SpMUS81-EME1 complexes that were purified as tetrameric complexes. The presence of two active sites supports the predicted nick-counternick mechanism (Gaskell et al., 2007).

In this work, though they were expressed in *E. coli*, the purified AtMUS81-AtEME1A and AtMUS81-AtEME1B preparations were able to cleave the nXO and XO HJ. The activity of both homologous complexes with the nXO structure was used as a standardization (like in Gaskell et al., 2007) to be able to compare their activities on the intact XO and the 3′-flap.

For yeasts, it was shown that the nXO structure is the preferred substrate over the XO structure; the nXO can be processed both with native and recombinant preparations of the protein complexes (Gaillard et al., 2003; Osman et al., 2003; Fricke et al., 2005; Gaskell et al., 2007; Ehmsen and Heyer, 2008). For AtMUS81-EME1A and AtMUS81-EME1B, we also observed a higher activity using the nXO substrate compared to the XO substrate, as indicated by the reaction time and the enzyme concentration needed for detectable activity. One possible explanation for this result is that the presence of the nick in the junction of the nHJ makes it a more flexible structure than the XO, so that after binding of the enzymatic complex, the junction is optimally positioned in the catalytic site of MUS81 to resolve the HJ into duplex structures with gaps and flaps. A distortion of the HJ-DNA structure upon binding to both complex partners HsMUS81 and HsEME1 could be observed so that the positions of the endonucleolytic cleavage were located several bases adjacent to the 5′ junction (Chang et al., 2008).

In this work, we were able to show that both AtMUS81-AtEME1A and AtMUS81-AtEME1B display identical cleavage patterns for nXO and the 3′-flap substrates. AtMUS81-AtEME1A prefers the position of four nucleotides 5′ of the junction point with XO. A similar preference for the position of four nucleotides 5′ of the junction point of XO could not be detected with the AtMUS81-AtEME1B complex. Thus, the AtMUS81-AtEME1A complex is more likely to perform symmetric cuts that could be religated. This might be of importance regarding CO formation. It has been postulated that nonsymmetric cuts are primarily resolved into COs (Ip et al., 2008). Deviations in the cleavage sites could result from differences in the amino acid sequences of the AtEME1 homologs that might affect substrate specificity and sequence preferences. It was postulated that differences in the helix hairpin helix motifs could determine substrate specificity in XPF/MUS81 family members (Ciccia et al., 2008).

The results presented in this article demonstrate that the AtMUS81-AtEME1A and AtMUS81-AtEME1B complexes possess characteristics for the resolution of HJs and are consistent with these endonuclease complexes being involved in DNA recombination and repair processes in Arabidopsis.

MATERIALS AND METHODS

RNA Extraction and RT-PCR of AtEME1A and AtEME1B

RNA from young Arabidopsis (*Arabidopsis thaliana* '*columbia*') plantlets was isolated using the RNeasy Plant Mini Kit from Qiagen according to the instructions of the manufacturer. RT was performed according to the SMART protocol from CLONTECH (Heidelberg) using 2 μg of total RNA. The cDNA produced was used for PCRs with primers located upstream and downstream of the coding regions of both genes.

Primers used for RT-PCR of AtEME1A were EME1A-ATG, 5′-ATGAGC-GATTTCATTTTGATC-3′, and EME1A-stop, 5′-CTAAATTAAGTCAGATG-GAGGAAG-3′. Primers used for RT-PCR of AtEME1B were EME1B-C

(upstream of the ATG codon), 5′-CATCATCTTCCTCGATAGTC-3′; and EME1B-RA (downstream of the stop codon), 5′-CAGTCTCCAATGACGTCTG-3′.

Cloning

For coexpression, the *MUS81* (At4g30870) ORF of Arabidopsis was cloned into MCS-1 of the pETDuet-1 vector with the ORF of *AtEME1A* (At2g21800) or *AtEME1B* (At2g22140) in MCS-2. A mutated form of AtMUS81 (as in Boddy et al., 2001) was constructed by introducing two point mutations (by overlap extension) in the catalytic center of the *AtMUS81*-ORF (AERKxxDD); these mutations change the amino acids at positions 470 and 471 from Asp (D) to Ala (A), yielding AtMUS81(D470-471A), using the following primer pairs: 5′-AGGAAGAACGTTGCTGCTATGCGCTCATCA-3′ and 5′-TGCTGTCGACTCATTCACCCCAAACTAAC-3′, and 5′-TGATGAGCGCATAGCAGCAACGTTCTTCCT-3′ and 5′-TGCTAGATCTTGATGACGAGAGACGGGTAC-3′, respectively (point mutations are underlined). The pETDuet-1 vector was then modified by deleting the existing S-tag using *Kpn*I and *Xma*JI and introducing a StrepII-tag adaptor composed of the two oligonucleotides 5′-CAGTGCTTGGAGCCACCCGCAGTTCGAAAAATAAC-3′ and 5′-CTAGGTTATTTTTCGAACTGCGGGTGGCTCCAAGCACTGGTAC-3′; the final products encoded $_{His}$AtMUS81-AtEME1A/1B$_{StrepII}$ and $_{His}$AtMUS81(D470-471A)-AtEME1A/1B$_{StrepII}$. The *AtEME1B*-ORF bears a change at base pair position 419 that changes an Asn at position 139 to Ser.

Expression

$_{His}$AtMUS81-AtEME1A/1B$_{StrepII}$ and $_{His}$AtMUS81(D470-471A)-AtEME1A/1B$_{StrepII}$ were overexpressed in *Escherichia coli* BL21(DE3). Induction was performed with 1 mM isopropylthio-β-galactoside for 6 h at 21°C and 200 rpm. Cells were collected by centrifugation.

Protein Purification

All purification steps were performed at 4°C. The frozen cell pellets of 750-mL cultures of bacteria were resuspended in 30 mL of buffer A (100 mM Tris-HCl, 100 mM KCl, 1 mM dithiothreitol [DTT], and 0.1% Tween 20, pH 7.0). The cells were lysed with the addition of 0.1 mg/mL lysozyme for 45 min on ice followed by sonication. The lysate was centrifuged for 30 min at 40,000*g* and 4°C, and the supernatant was filtered using a GF/PET membrane. After the addition of 2 μg/mL avidin, the clear lysate was loaded onto a self-packed 4 mL Strep-Tactin Superflow (IBA) gravity column equilibrated with buffer A. After washing with 25 mL of buffer A, the proteins were eluted stepwise with 10 mL of buffer B (100 mM Tris-HCl, 50 mM KCl, 1 mM DTT, 0.1% Tween 20, and 3 mM desthiobiotin, pH 7.0). After the elution fractions were pooled and the volume was adjusted to 10 mL with buffer B, the buffer was exchanged to buffer C (50 mM Na_2HPO_4, 200 mM KCl, 40 mM imidazole, and 10% glycerol, pH 7.0) using PD10 columns (GE Healthcare) equilibrated with buffer C. The eluate was loaded onto an equilibrated 1 mL HiTrap Chelating HP column (GE Healthcare) with Cu^{2+} as the ligand at a flow rate of 0.5 mL/min using a low-pressure liquid chromatography system (BioLogic LP; Bio-Rad Laboratories). After washing the column with 35 to 45 mL of buffer C (flow rate 1 mL/min), the proteins were eluted with buffer D (buffer C plus 400 mM imidazole; 20 mL, flow rate 0.5 mL/min). The buffer of the peak fractions was exchanged to buffer E (100 mM Tris-HCl and 25 mM KCl, pH 7.0) using NAP5 columns (GE Healthcare) and the end fractions were mixed with 50% glycerol, a protease inhibitor mix (Serva), 5 mM EDTA, 5 mM $MgCl_2$, 1 mM DTT, and 0.1% Tween 20 and stored at −20°C. The protein complexes were identified by colloidal Coomassie-stained (Neuhoff et al., 1988) SDS-PAGE gels and western blot and quantified with ImageJ software (http://rsb.info.nih.gov/ij/) using BSA (Bio-Rad) as a standard.

DNA Substrates

All substrates were prepared by annealing the appropriate combinations of the respective oligonucleotides and purified by 10% TBE native gel electrophoresis and subsequent electroelution in TB-$MgCl_2$ buffer (44.5 mM Tris-Base, 44.5 mM boric acid, and 5 mM $MgCl_2$) using D-Tube Dialyzers (Merck). The same oligonucleotide sequences were used as previously described (Boddy et al., 2001; Gaillard et al., 2003). Four different XO and nXO junctions (XO-1/XO-2/XO-3/XO-4 and nXO-1/nXO-2/nXO-3/nXO-4), each 5′ labeled on a different oligonucleotide, were prepared using [γ-^{32}P]ATP (6000 Ci/mmol; Hartmann Analytic) and T4 polynucleotide kinase (NEB).

Endonuclease Assays

Reactions (20 μL) contained 50 fmol ^{32}P-labeled substrate (2.5 nM) in 1× reaction buffer (25 mM Tris-HCl, 1 mM $MgCl_2$ [unless otherwise indicated], 100 μg/mL BSA, and 1 mM DTT); the reactions were performed at 37°C and started by mixing the enzyme with the other reaction components. Cleavage reactions with the XO substrates contained 10/6.4 ng (6.74/4.27 nM) purified AtMUS81-AtEME1A or AtMUS81-AtEME1B protein or 2/1.3 ng (1.35/0.87 nM) AtMUS81-AtEME1A or AtMUS81-AtEME1B protein, respectively, for reactions with nXO and 3′-flap substrates. For time-course experiments, the reaction volume was increased, and 20-μL aliquots were removed at time points 30, 60, 120, 180, and 240 min; the reactions were stopped with the addition of 10 μL TBE-urea buffer (89 mM Tris-HCl, 89 mM boric acid, 2 mM EDTA, 7 M urea, 12% Ficoll, 0.01% bromphenol blue, and 0.02% xylene-cyanol FF) followed by denaturation for 5 min at 95°C. For the 3′-flap and nXO substrates, time points 2.5, 5, 10, 30, and 60 min were tested. Reactions that were allowed to incubate for the maximum time with the protein complexes AtMUS81(D470-471A)-AtEME1A and AtMUS81(D470-471A)-AtEME1B or without any enzyme were run in parallel and were subtracted as background from each indicated value.

Eight microliters of each sample were loaded on a 7 M urea 20% TBE-PAGE denaturing sequencing gel with constant power (60 W) and a maximum voltage of 2,500 V at 50°C. The gels were vacuum dried for 2 h at 80°C and 300 mbar on cellophane sheet and exposed for about 90 min to a phosphor imager screen. The detection was performed by autoradiography using the FUJIFILM BAS-1500 reader. For native PAGE, the reaction was stopped with a third volume of stop solution (50 mM EDTA, 0.6% SDS, 20% glycerol, 0.1% xylene-cyanol FF, and 0.1% bromphenol blue), 10 μL of each sample was run on a 10% TBE-PAGE gel at 4°C, and detection was performed using the Instant Imager (Canberra Packard Company).

Sequence data from this article can be found in the GenBank/EMBL data libraries under accession numbers AB177892 (AtMUS81), FJ161970 (AtEME1B), and FJ936556 (AtEME1A).

Supplemental Data

The following materials are available in the online version of this article.

Supplemental Figure S1. SDS-PAGE analysis of purified AtMUS81-AtEME1A and AtMUS81-AtEME1B endonuclease complexes.

Supplemental Table S1. Summarized data of real-time PCR experiments analyzing AtMUS81, AtEME1A, and AtEME1B expression in different tissues.

ACKNOWLEDGMENTS

We thank Marion Förschle for technical assistance and D. Wedlich for providing the BAS-1500 reader.

Received February 9, 2009; accepted March 31, 2009; published April 1, 2009.

LITERATURE CITED

Abraham J, Lemmers B, Hande MP, Moynahan ME, Chahwan C, Ciccia A, Essers J, Hanada K, Chahwan R, Khaw AK, et al (2003) Eme1 is involved in DNA damage processing and maintenance of genomic stability in mammalian cells. EMBO J **22:** 6137–6147

Bastin-Shanower SA, Fricke WM, Mullen JR, Brill SJ (2003) The mechanism of Mus81-Mms4 cleavage site selection distinguishes it from the homologous endonuclease Rad1-Rad10. Mol Cell Biol **23:** 3487–3496

Berchowitz LE, Francis KE, Bey AL, Copenhaver GP (2007) The role of AtMUS81 in interference-insensitive crossovers in *A. thaliana*. PLoS Genet **3:** e132

Blais V, Gao H, Elwell CA, Boddy MN, Gaillard PH, Russell P, McGowan

CH (2004) RNA interference inhibition of Mus81 reduces mitotic recombination in human cells. Mol Biol Cell **15:** 552–562

Boddy MN, Gaillard PH, McDonald WH, Shanahan P, Yates JR III, Russell P (2001) Mus81-Eme1 are essential components of a Holliday junction resolvase. Cell **107:** 537–548

Boddy MN, Lopez-Girona A, Shanahan P, Interthal H, Heyer WD, Russell P (2000) Damage tolerance protein Mus81 associates with the FHA1 domain of checkpoint kinase Cds1. Mol Cell Biol **20:** 8758–8766

Chang JH, Kim JJ, Choi JM, Lee JH, Cho Y (2008) Crystal structure of the Mus81-Eme1 complex. Genes Dev **22:** 1093–1106

Chen XB, Melchionna R, Denis CM, Gaillard PH, Blasina A, Van de Weyer I, Boddy MN, Russell P, Vialard J, McGowan CH (2001) Human Mus81-associated endonuclease cleaves Holliday junctions in vitro. Mol Cell **8:** 1117–1127

Ciccia A, Constantinou A, West SC (2003) Identification and characterization of the human mus81-eme1 endonuclease. J Biol Chem **278:** 25172–25178

Ciccia A, Ling C, Coulthard R, Yan Z, Xue Y, Meetei AR, Laghmaniel H, Joenje H, McDonald N, de Winter JP, et al (2007) Identification of FAAP24, a Fanconi anemia core complex protein that interacts with FANCM. Mol Cell **25:** 331–343

Ciccia A, McDonald N, West SC (2008) Structural and functional relationships of the XPF/MUS81 family of proteins. Annu Rev Biochem **77:** 259–287

Constantinou A, Chen XB, McGowan CH, West SC (2002) Holliday junction resolution in human cells: two junction endonucleases with distinct substrate specificities. EMBO J **21:** 5577–5585

Copenhaver GP, Housworth EA, Stahl FW (2002) Crossover interference in Arabidopsis. Genetics **160:** 1631–1639

de los Santos T, Hunter N, Lee C, Larkin B, Loidl J, Hollingsworth NM (2003) The Mus81/Mms4 endonuclease acts independently of double-Holliday junction resolution to promote a distinct subset of crossovers during meiosis in budding yeast. Genetics **164:** 81–94

de los Santos T, Loidl J, Larkin B, Hollingsworth NM (2001) A role for MMS4 in the processing of recombination intermediates during meiosis in *Saccharomyces cerevisiae*. Genetics **159:** 1511–1525

Doe CL, Ahn JS, Dixon J, Whitby MC (2002) Mus81-Eme1 and Rqh1 involvement in processing stalled and collapsed replication forks. J Biol Chem **277:** 32753–32759

Ehmsen KT, Heyer WD (2008) *Saccharomyces cerevisiae* Mus81-Mms4 is a catalytic, DNA structure-selective endonuclease. Nucleic Acids Res **36:** 2182–2195

Fricke WM, Bastin-Shanower SA, Brill SJ (2005) Substrate specificity of the *Saccharomyces cerevisiae* Mus81-Mms4 endonuclease. DNA Repair (Amst) **4:** 243–251

Gaillard PH, Noguchi E, Shanahan P, Russell P (2003) The endogenous Mus81-Eme1 complex resolves Holliday junctions by a nick and counternick mechanism. Mol Cell **12:** 747–759

Gaskell LJ, Osman F, Gilbert RJ, Whitby MC (2007) Mus81 cleavage of Holliday junctions: a failsafe for processing meiotic recombination intermediates? EMBO J **26:** 1891–1901

Hanada K, Budzowska M, Modesti M, Maas A, Wyman C, Essers J, Kanaar R (2006) The structure-specific endonuclease Mus81-Eme1 promotes conversion of interstrand DNA crosslinks into double-strands breaks. EMBO J **25:** 4921–4932

Hartung F, Blattner FR, Puchta H (2002) Intron gain and loss in the evolution of the conserved eukaryotic recombination machinery. Nucleic Acids Res **30:** 5175–5181

Hartung F, Suer S, Bergmann T, Puchta H (2006) The role of AtMUS81 in DNA repair and its genetic interaction with the helicase AtRecQ4A. Nucleic Acids Res **34:** 4438–4448

Hartung F, Suer S, Puchta H (2007a) Two closely related RecQ helicases have antagonistic roles in homologous recombination and DNA repair in *Arabidopsis thaliana*. Proc Natl Acad Sci USA **104:** 18836–18841

Hartung F, Wurz-Wildersinn R, Fuchs J, Schubert I, Suer S, Puchta H (2007b) The catalytically active tyrosine residues of both SPO11-1 and SPO11-2 are required for meiotic double-strand break induction in *Arabidopsis*. Plant Cell **19:** 3090–3099

Higgins JD, Buckling EF, Franklin FC, Jones GH (2008) Expression and functional analysis of AtMUS81 in Arabidopsis meiosis reveals a role in the second pathway of crossing-over. Plant J **54:** 152–162

Holloway JK, Booth J, Edelmann W, McGowan CH, Cohen PE (2008) MUS81 generates a subset of MLH1-MLH3-independent crossovers in mammalian meiosis. PLoS Genet **4:** e1000186

Interthal H, Heyer WD (2000) MUS81 encodes a novel helix-hairpin-helix protein involved in the response to UV- and methylation-induced DNA damage in *Saccharomyces cerevisiae*. Mol Gen Genet **263:** 812–827

Ip SC, Rass U, Blanco MG, Flynn HR, Skehel JM, West SC (2008) Identification of Holliday junction resolvases from humans and yeast. Nature **456:** 357–361

Kaliraman V, Mullen JR, Fricke WM, Bastin-Shanower SA, Brill SJ (2001) Functional overlap between Sgs1-Top3 and the Mms4-Mus81 endonuclease. Genes Dev **15:** 2730–2740

Kobbe D, Blanck S, Demand K, Focke M, Puchta H (2008) AtRECQ2, a RecQ-helicase homologue from Arabidopsis thaliana, is able to disrupt different recombinogenic DNA-structures in vitro. Plant J **55:** 397–405

McPherson JP, Lemmers B, Chahwan R, Pamidi A, Migon E, Matysiak-Zablocki E, Moynahan ME, Essers J, Hanada K, Poonepalli A, et al (2004) Involvement of mammalian Mus81 in genome integrity and tumor suppression. Science **304:** 1822–1826

Mullen JR, Kaliraman V, Ibrahim SS, Brill SJ (2001) Requirement for three novel protein complexes in the absence of the Sgs1 DNA helicase in *Saccharomyces cerevisiae*. Genetics **157:** 103–118

Neuhoff V, Arold N, Taube D, Ehrhardt W (1988) Improved staining of proteins in polyacrylamide gels including isoelectric focusing gels with clear background at nanogram sensitivity using Coomassie Brilliant Blue G-250 and R-250. Electrophoresis **9:** 255–262

Nishino T, Ishino Y, Morikawa K (2006) Structure-specific DNA nucleases: structural basis for 3D-scissors. Curr Opin Struct Biol **16:** 60–67

Nishino T, Komori K, Ishino Y, Morikawa K (2003) X-ray and biochemical anatomy of an archaeal XPF/Rad1/Mus81 family nuclease: similarity between its endonuclease domain and restriction enzymes. Structure **11:** 445–457

Odagiri N, Seki M, Onoda F, Yoshimura A, Watanabe S, Enomoto T (2003) Budding yeast mms4 is epistatic with rad52 and the function of Mms4 can be replaced by a bacterial Holliday junction resolvase. DNA Repair (Amst) **2:** 347–358

Oh SD, Lao JP, Taylor AF, Smith GR, Hunter N (2008) RecQ helicase, Sgs1, and XPF family endonuclease, Mus81-Mms4, resolve aberrant joint molecules during meiotic recombination. Mol Cell **31:** 324–336

Osman F, Dixon J, Doe CL, Whitby MC (2003) Generating crossovers by resolution of nicked Holliday junctions: a role for Mus81-Eme1 in meiosis. Mol Cell **12:** 761–774

Puchta H (2005) The repair of double-strand breaks in plants: mechanisms and consequences for genome evolution. J Exp Bot **56:** 1–14

Schranz ME, Mitchell-Olds T (2006) Independent ancient polyploidy events in the sister families Brassicaceae and Cleomaceae. Plant Cell **18:** 1152–1165

Taylor ER, McGowan CH (2008) Cleavage mechanism of human Mus81-Eme1 acting on Holliday-junction structures. Proc Natl Acad Sci USA **105:** 3757–3762

Trowbridge K, McKim K, Brill SJ, Sekelsky J (2007) Synthetic lethality of Drosophila in the absence of the MUS81 endonuclease and the DmBlm helicase is associated with elevated apoptosis. Genetics **176:** 1993–2001

Tuteja N, Singh MB, Misra MK, Bhalla PL, Tuteja R (2001) Molecular mechanisms of DNA damage and repair: progress in plants. Crit Rev Biochem Mol Biol **36:** 337–397

Whitby MC (2005) Making crossovers during meiosis. Biochem Soc Trans **33:** 1451–1455

Whitby MC, Osman F, Dixon J (2003) Cleavage of model replication forks by fission yeast Mus81-Eme1 and budding yeast Mus81-Mms4. J Biol Chem **278:** 6928–6935